Journal of Catalysis **181,** 271–279 (1999)
Article ID jcat.1998.2301, available online at http://www.idealibrary.com on IDEAL®

Methanol Synthesis from CO_2, CO, and H_2 over Cu(100) and Ni/Cu(100)

Jesper Nerlov[1] and Ib Chorkendorff

Center for Atomic-scale Materials Physics (CAMP), Physics Department, Building 307, Technical University of Denmark, DK-2800 Lyngby, Denmark

Received July 16, 1998; revised October 8, 1998; accepted October 8, 1998

The catalytic activity of Cu(100) and Ni/Cu(100) with respect to the methanol synthesis from various mixtures containing CO_2, CO, and H_2 have been studied in a combined UHV/high pressure cell apparatus at reaction conditions, $P_{tot} = 1.5$ bar and $T = 543$ K. For the clean Cu(100) surface it is found that admission of CO to a reaction mixture containing CO_2 and H_2 does not lead to an increase in the rate of methanol formation, which indirectly suggests that the role of CO in the industrial methanol process relates to the change in reduction potential of the synthesis gas. For the Ni/Cu(100) surface it is found that Ni does not promote the rate of methanol formation from mixtures containing CO_2 and H_2. In opposition, admission of CO to the reaction mixture leads to a significant increase in the rate of methanol formation with a turnover frequency/Ni site $\sim 60 \times$ the turnover frequency/Cu site at Ni coverages below 0.1 ML making it a rather substantial promoting effect. It is found that the admission of CO to the synthesis gas creates segregation of Ni to the surface, whereas this is not the case for a reaction involving CO_2 and H_2. It is suggested that CO acts strictly as a promotor in the system and we ascribe the increase in activity to a promotion through gas phase induced surface segregation of Ni.

Key Words: **methanol synthesis; CO; CO_2; H_2; nickel promotion; segregation.**

1. INTRODUCTION

Industrially, methanol is synthesised from a mixture of hydrogen, carbon dioxide, and carbon monoxide (synthesis gas) at pressures of 50–100 bar and temperatures of 500–550 K over $Cu/ZnO/Al_2O_3$ catalysts. It has been shown by isotope labelling experiments that CO_2 is the main source of carbon in methanol (MeOH) formed from synthesis gas (1–3) and that the rate of methanol formation obtained from CO_2/H_2 mixtures over a Cu(100) single crystal can account for the activity of real catalysts (4, 5). Other vinicial planes af copper single crystals and poly crystalline copper have lately been investigated and are also found to synthesize methanol in similar amounts (6, 7). This strongly implies that the synthesis takes place through the reaction

$$CO_2 + 3H_2 \rightleftharpoons CH_3OH + H_2O,$$

whereas CO is coupled to this reaction through the reverse water–gas shift (RWGS) reaction:

$$CO_2 + H_2 \rightleftharpoons CO + H_2O.$$

Nonetheless, the role of CO is still a matter of controversy. For instance Clausen *et al*. has shown by means of *in-situ* extended X-ray absorbtion fine structure (EXAFS) studies (8) that reversible changes in the morphology of the Cu particles occur as the reduction potential of the gas mixture is varied. This was recently included in a dynamical microkinetic model of the methanol synthesis (9), whereby a much better description of kinetic measurements over working catalysts was obtained. In this way the increase in activity of a $CO/CO_2/H_2$ mixture compared to a CO_2/H_2 mixture over real catalysts was ascribed to an area effect. This point of view was to some extent questioned by Yoshihara and Campbell (6) who, in a combined UHV/high-pressure-cell (HPC) study, found that addition of CO to the synthesis gas led to an increase in the rate of methanol formation over Cu(110).

In order to address these somewhat contradictory results we have performed additional UHV/HPC studies of methanol formation from mixtures of CO, CO_2, and H_2 over a single crystalline copper surface. We find that addition of CO to a CO_2/H_2 mixture does not lead to changes of the rate of MeOH formation over Cu(100). This result was, however, only obtained after extreme precautions were taken to avoid Ni contamination of the surface during the reaction in the high-pressure cell (the cell was rebuilt in steel which did not contain Ni). Comparison with the results of Ref. (6) shows that Ni contamination may very well have been the reason for the increase in reactivity of the CO-containing gas mixture in that work.

Therefore, we have also studied the influence of Ni deposition on the rate of MeOH formation from mixtures of CO, CO_2, and H_2 over Cu(100). We find that deposition of submonolayer quantities of Ni does not lead to any change in the rate of MeOH formation from mixtures of CO_2 and H_2, just as MeOH cannot be formed in measurable amounts from mixtures of CO and H_2. On the other hand, the rate of MeOH formation from mixtures of CO, CO_2, and H_2 increases dramatically upon deposition of submonolayer

[1] Corresponding author. Present address: Haldor Topsøe Research Laboratories, DK-2800 Lyngby, Denmark.

0021-9517/99 $30.00

quantities of Ni with the TOF/Ni site $\sim 60 \times$ TOF/Cu site for the initially deposited Ni. By separate adsorption/desorption experiments it is found that Ni goes to the subsurface upon annealing at the reaction temperature. However, by introducing a sufficient partial pressure of CO (in the mbar range) Ni can be maintained at the surface. This is due to the stronger bonding of CO to Ni, as compared to Cu. In this way we ascribe the increase in activity to a gas phase induced change in surface composition introduced by CO. It is suggested that the role of CO is strictly promoting contrary to being hydrogenated directly into methanol.

2. EXPERIMENTAL

All experiments were performed in a conventional stainless steel UHV chamber equipped with a high-pressure cell (HPC). The UHV system has been described in detail elsewhere (4, 10). Initial experiments with CO clearly demonstrated that special precautions had to be taken. The high-pressure cell was therefore subject to some changes. First it has been rebuilt in steel which only contains traces of Ni and the cromel/alumel thermo-couple was replaced by a W/Re thermo-couple. This was done in order to avoid formation of nickel carbonyls (mainly $Ni(CO)_4$) in the cell at elevated CO pressures, since it was found that these carbonyls decompose on the sample, leading to severe Ni contamination of the surface. Even so, a small residual Ni contamination level could not be completely avoided. Whether this originated from the bulk of the Cu crystal, from carbonyls present in the synthesis gas, or, alternatively, from Ni-containing feedthroughs within the HPC, is not clear. A contamination level of 0.001 ML Ni/h at $P_{CO} = 100$ mbar and $T_{sample} = 543$ K was, however, regarded as insignificant for the interpretation of the obtained data. However, the contamination level depends strongly on the partial pressure of CO and more than 0.01 ML Ni/h was obtained after reaction at a CO partial pressure of 500 mbar. This limits the experimental regime to the 100 mbar range on which we have focused in the present work. The more technical details concerning the precautions taken against Ni contamination from both the steel of the HPC but also Ni containing feedthroughs will be dealt with in more detail elsewhere (11).

The second modification relates to the analysis of the reaction mixture. In the present work the gas composition was studied by means of a gas chromatograph (GC), instead of the previously used quadrapole mass spectrometer (QMS). Both a thermal conduction and a flame ionization detector were employed which allowed quantitative detection of both reaction products, as well as the components of the synthesis gas. The gases used were H_2 (ALFAX N57), CO_2 (ALFAX N48), and CO (ALFAX N47). Both H_2 and CO_2 were subject to additional purification as described in Ref. (4). CO was led through a Cu coil which was frozen at 77 K before introduction to the HPC. This was done mainly to remove $Ni(CO)_4$ which, as described above, is a critical contaminant for the present experiments.

The Cu(100) crystal was cut, polished on both sides, and prepared as described in Ref. (10). It was mounted on 0.5-mm gold wires which were also used for resistively heating. The temperature was measured using a W/Re-type thermocouple, free of Ni. Ni was evaporated by resistively heating a tungsten filament which had thin Ni wire wrapped around it. In the experiments reported here equal amounts of Ni were deposited on both faces of the crystal and the coverages given below are the mean values. A deviation of 10% from the mean value was allowed for. The components of the synthesis gas were introduced one at the time into the HPC following the sequence CO_2, CO, and H_2. The gas mixture was then allowed to mix for 15 min before the reaction started. The reaction was run in batch mode for $\Delta t = 45$ min at $T = 543$ K and $P_{tot} = 1.5$ bar. The walls of the HPC and the tubes in the setup for admittance and removal of the gases were kept at $T = 350$ K in order to avoid adsorption of MeOH, which would lead to memory effects. Two experiments were never performed the same day and the amount of MeOH present in a blind experiment (involving pure H_2) carried out the day after a synthesis experiment was below the detection limit of our system. After the reaction the sample was allowed to cool to $T \sim 333$ K before the gas was pumped out. This is slightly below the temperature of the HPC and can only be obtained because the electrical feedthroughs was air cooled during all experiments. The post-reaction surface was then investigated by XPS and TPD. The final temperature of the TPD spectra were 573 K except for TPD spectra of pure CO exposure (Fig. 6) which were heated to the reaction temperature ($T = 543$ K).

The rate of MeOH formation over Cu(100) from CO_2/H_2 mixtures has previously been investigated in our system (4). In that case methanol was detected by means of a QMS. Calibration of the present GC signal with respect to the amount of methanol synthesized was then obtained performing experiments at the same conditions as in (4). This allowed us to relate directly a given GC signal to a turnover frequency/site $*$ s (TOF). For convenience we have defined one site in the present work as one Cu atom and anticipated that 1 ML of Ni atoms is equal to that of Cu (in Ref. (4) one site corresponded to two Cu atoms, but as we will deal with reactivity/Ni atom in this work, we have changed the unit). It was found in a separate experiment that the two faces of the crystal accounted for approximately 2/3 of the MeOH formed during a synthesis over clean Cu(100), just as it was assumed that Ni was only deposited on the faces of the crystal (excluding the rim). Both for the experiments involving the clean surface and those involving Ni deposition the TOFs given below specifically relates to sites on

the two faces of the crystal. For the Ni/Cu(100) system the TOF is considered as

$$TOF = TOF_{\mathrm{Ni_{site}}} * \theta_{\mathrm{Ni}} + TOF_{\mathrm{Cu_{site}}} * \theta_{\mathrm{Cu(100)}} \qquad [1]$$

which allow for a determination of $TOF_{\mathrm{Ni_{site}}}$.

3. RESULTS

3.1. Cu(100)

Figure 1 shows the rate of methanol formation over clean Cu(100) for various mixtures of CO_2 and H_2 with or without addition of 100 mbar of CO ($P_{H_2} = 1500$ mbar $- P_{CO} - P_{CO_2}$, $T = 543$ K). In both cases we obtain a monotonically increasing rate for increasing pressures of CO_2. This behavior is accordance with the kinetic measurements and modelling performed in Refs. (4, 12) for reaction mixtures of CO_2 and H_2 over Cu(100). Here (Refs. (4, 12)) a maximum value for the MeOH rate was obtained around a molefraction of CO_2 of 0.3–0.5 (corresponding to $P_{CO_2} = 450$–750 mbar). The variations of the MeOH rate obtained in the two cases given in Fig. 1 are considered to be within the error bar of the measurements and, consequently, it appears that CO has no measureable influence on the rate of MeOH formation at these conditions. This finding is somewhat in opposition to what was observed in Ref. (6), where a small increase was observed upon admission of CO ($P_{CO} = 100$–1000 mbar). Furthermore, it follows from Fig. 1 that the rate of MeOH formation from a mixture of 100 mbar CO and 1400 mbar H_2 (with no CO_2 present) at the present conditions is below the detection limit of our system (TOF/site $* s < 1 * 10^{-6}$). This is taken as further evidence for the idea that MeOH is formed from CO_2 and H_2 over Cu-based catalysts as discussed in the Introduction.

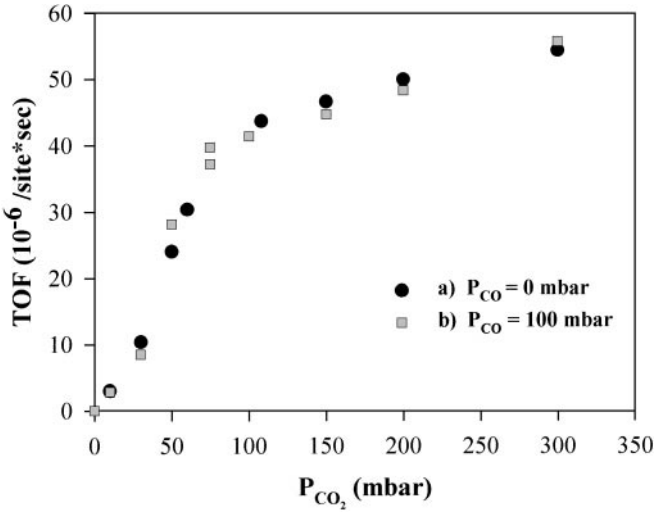

FIG. 1. The rate of MeOH formation over Cu(100) at $P_{tot} = 1.5$ bar and $T = 543$ K as function of the partial pressure of CO_2: (a) a mixture of CO_2 and H_2; (b) a mixture of 100 mbar CO, CO_2, and H_2.

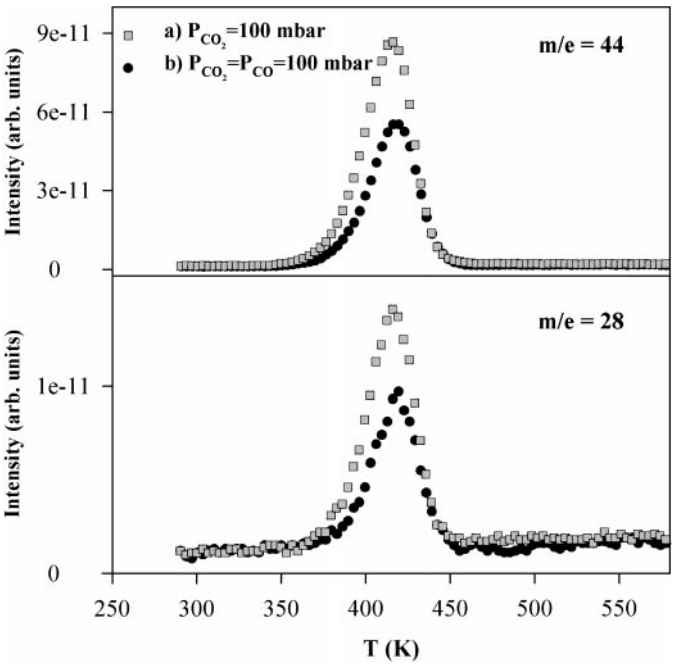

FIG. 2. TPD spectra (m/e = 28 (lower panel) and m/e = 44 (upper panel)) obtained after pump out of synthesis gas at 333 K: (a) a mixture of 100 mbar CO_2 and 1400 mbar H_2; (b) a mixture of 100 mbar CO, 100 mbar CO_2, and 1300 mbar H_2.

The postreaction surface was examined by XPS and TPD. In the TPD spectra only one desorbing species, namely CO_2 at $T = 420$ K, could be observed both from CO_2/H_2 and $CO/CO_2/H_2$ mixtures as shown in Fig. 2. In accordance with previous data (13), this is attributed to disproportionation of formate to CO_2 and H_2. Owing to a high background of H_2 following the reaction in the HPC we could not resolve the expected signal from desorbing hydrogen. Furthermore, it should be noted that in opposition to what was observed in Ref. (6) for reaction of $CO/CO_2/H_2$ mixtures over Cu(110) at similar conditions no CO-related TPD could be detected at $T \sim 370$ K from the samples exposed to 100 mbar of CO (the weak peak observed at m/e = 28 in Fig. 2 is due to cracking of CO_2 in the QMS). With respect to the XPS signal two carbon features ($E_B = 285$ eV and $E_B = 289$ eV) and one oxygen feature ($E_B = 531.5$ eV) could be observed. The oxygen feature and the high-binding-energy carbon feature dissapear during the TPD experiment and they are attributed to be related to formate while the low-binding energy feature remains. The latter is attributed to graphite formed on the surface during the reaction; but considering that the coverage of this species never exceeded 5% of a monolayer and that it did not seem to influence the methanol synthesis rate (the rate was not sensitive to variations of graphite concentration in this limit), it is considered to be insignificant to the data interpretation.

3.2. Ni/Cu(100)

In order to study the influence of Ni on the MeOH synthesis over Cu(100) a calibration of the Ni coverage was carried out. We chose to estimate the surface coverage of Ni from the area of the CO TPD peak obtained after reaction in the high pressure cell at $T = 543$ K, $\Delta t = 45$ min, involving a mixture of 100 mbar CO, 30 mbar CO_2, and 1370 mbar H_2. We define 1 ML as the saturation point of the CO desorption peak. This agrees within 15% with the $I(Ni_{2p})/I(Cu_{2p})$ intensity ratio one would expect from a simple model incorporating photoionization cross sections of Cu_{2p} and Ni_{2p} levels and the attenuation length of Cu_{2p} photoelectrons. In cases where a TPD was not performed this model was used for determination of the coverages by including a scaling factor that takes this deviation into account. It is clear from Fig. 3 that the CO uptake in the experiment involving reaction in the high pressure cell is essentially linear in Ni coverage up to the point where saturation is obtained. The CO uptake obtained after exposing a freshly deposited Ni film to 10 L of CO at RT is also shown in Fig. 3. Here we observe a fairly linear increase in the CO TPD signal at coverages below $\theta_{Ni} \sim 0.3$ ML. Above this point the increase in CO signal is obviously slower than for the surfaces which have been subject to exposures in the high-pressure cell. The CO signal continues to increase at Ni coverages above 1 ML and even at $\theta_{Ni} \sim 2$ ML the saturation level of CO is not reached.

Figure 4 (curve a) shows the rate of MeOH formation from a mixture of 30 mbar CO_2, 100 mbar CO, and 1370 mbar H_2 as a function of the Ni coverage. We observe a strong initial increase in activity as Ni is deposited. At $\theta_{Ni} \sim 0.2$ ML an increase in the MeOH production (per site) of more than 500% is obtained. Upon further deposition the rate appears to be fairly constant (a small decrease is observed). We may then ascribe the promotional effect to the presence of Ni at the surface and thereby relate the increase in the rate of MeOH formation to a TOF/Ni site. From the initial slope of the rate versus the coverage curve shown in Fig. 4 (curve a) we obtain for the initially deposited Ni a TOF/Ni site $\sim 60 *$ TOF/Cu site, making it a rather substantial promotional effect.

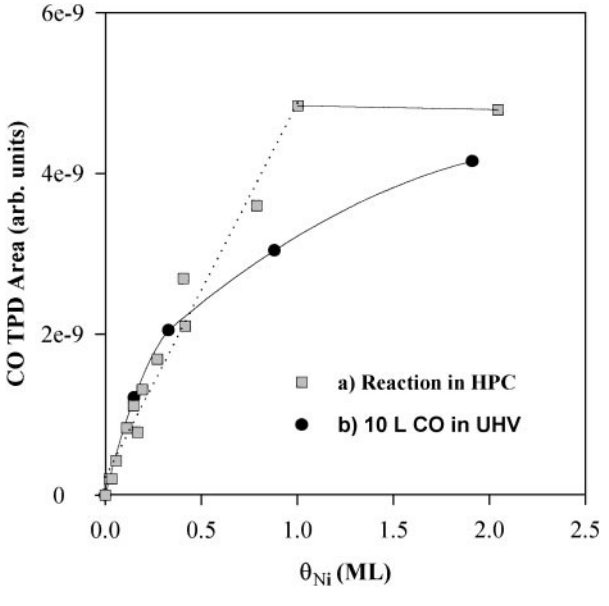

FIG. 3. The areas of CO TPD curves (m/e = 28) as function of Ni coverage obtained after (a) a reaction at 543 K involving 30 mbar CO_2, 100 mbar CO, and 1370 mbar H_2; (b) a dose of 10 L CO in UHV. 1 ML is defined as the coverage corresponding to saturation of the uptake of CO, as judged by the HPC experiments.

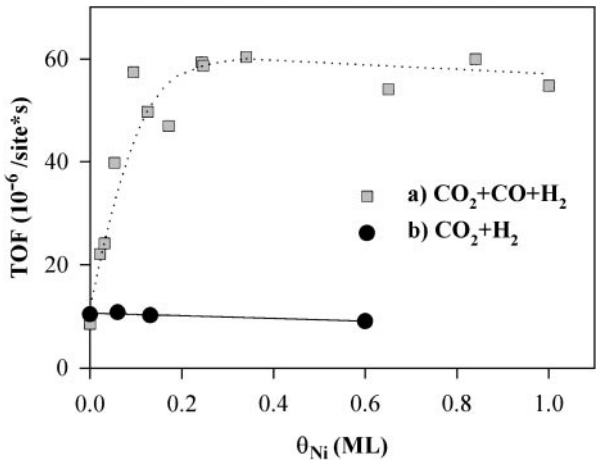

FIG. 4. The rate of MeOH formation over Ni/Cu(100) as function of the Ni coverage: (a) a mixture of 100 mbar CO, 30 mbar CO_2, and 1370 mbar H_2; (b) a mixture of 30 mbar CO_2 and 1470 mbar H_2.

Figure 4 (curve b) shows the rate of MeOH formation from a 30 mbar CO_2/1470 mbar H_2 mixture as a function of the Ni coverage. The influence of Ni is obviously negligible (a small decrease within the error bar of the measurements is observed). In the same manner the reactivity of a 100 mbar CO/1400 mbar H_2 mixture as a function of the Ni coverage was measured (not shown). As for the clean surface, the level of MeOH remained below the detection limit after Ni deposition in the submonolayer regime. Thus, we are obviously dealing with a synergy effect, where neither of the combinations (CO, CO_2, H_2), (CO_2, H_2, Ni), nor (CO, H_2, Ni) appears to effect the rate of MeOH formation, whereas the presence of all four components leads to a substantial increase in reactivity.

Considering that during the reaction that both Ni and CO are present at the surface one could expect disproportionation reactions to occur, leading to the deposition of carbon and/or methane formation. No carbon buildup beyond the low level always observed on the clean copper crystal (less than 5% of a monolayer graphite and dependent on the overall cleanliness of the cell) was observed in the postreaction XPS investigation. A weak increase of the methane signal could, however, be observed at the highest

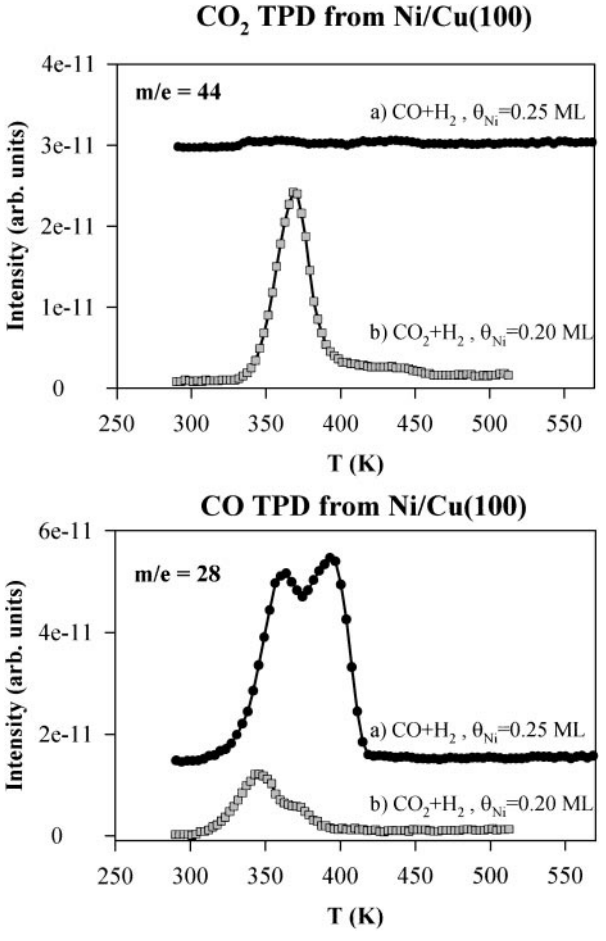

FIG. 5. TPD curves (m/e = 44, upper panel; m/e = 28, lower panel) obtained from Ni/Cu(100) surfaces after (a) a reaction involving 100 mbar CO and 1400 mbar H_2 over 0.25 ML Ni/Cu(100) and (b) a reaction involving 30 mbar CO_2 and 1470 mbar H_2 over 0.20 ML Ni/Cu(100).

Ni coverages. Due to a relative high and over time (days) a monotonously decreasing background of methane, which was independent of the status of the Cu crystal, it was not possible to quantify this signal. The weak dependency indicates that isolated Ni atoms in the low coverage regime are not capable of dissociating CO, whereas this possibility increases when bigger ensembles of Ni become possible at the high coverage.

Figure 5 shows the postreaction TPD spectra obtained after reactions of 30 mbar CO_2/1470 mbar H_2 over 0.20 ML Ni/Cu(100) and 100 mbar CO and 1400 mbar H_2 over 0.25 ML Ni/Cu(100). For the reaction involving CO and H_2 we observe CO-related peaks at $T = 360$ K and 390 K (Fig. 5 lower panel, curve a). Since CO does not adsorb at these conditions on clean Cu (according to Fig. 2), this feature is attributed to desorption of CO bonding to one or more Ni atoms. This is in accordance with Ref. (14), where CO desorption from various surface compositions of Ni/Cu alloys was studied. No CO_2-related TPD feature can be observed in this case (Fig. 5 upper panel, curve a). The corresponding XPS signal related to the presence of CO was observed at $E_B(C_{1s}) = 290$ eV and $E_B(O_{1s}) = 532.5$ eV, respectively.

For the reaction involving CO_2 and H_2 we also observe a CO-related TPD peak at $T \sim 345$ K (Fig. 5 lower panel, curve b). In addition a strong CO_2-related peak at $T \sim 370$ K is observed (Fig. 5 upper panel, curve b). This is attributed to decomposition of formate bonding to one (or more) Ni atoms. This is in accordance with the results of Ref. (15), where formate decomposition on Ni(110) was observed at $T = 330$ K. The C_{1s} and O_{1s} XPS spectra of the postreaction surfaces are consistent with combined emission from both CO and formate. It is somewhat unexpected that such a noticeable CO desorption peak is observed after reaction of CO_2 and H_2. In the postreaction GC analysis of the gas mixture only a very weak CO TPD signal could be observed. It is estimated that it amounts to a partial pressure of CO of approximately 0.2 mbar. It originates from the reverse water–gas-shift reaction which, as mentioned in the Introduction, runs parallel with the MeOH synthesis over Cu surfaces. It has been estimated that the RWGS reaction rate from CO_2/H_2 mixtures is about two orders of magnitude larger than for the MeOH synthesis (6) which is in good agreement with the magnitude of the observed signal.

With respect to the XPS observations it should be noted that neither in the present nor in the following case do we observe emission from chemisorbed oxygen, which would be situated at $E_B = 530$ eV. With the large pressures of H_2 and the very low dissociation rate of CO_2 (16, 17), we expect that oxygen originating from CO_2 dissociation most probably is hydrogenated to OH and water. Hence, we feel that it is safe to exclude the possibility of CO and O recombination as the origin of the low temperature CO_2 desorption peak.

The TPD spectra obtained after a reaction involving a mixture of 100 mbar CO, 30 mbar CO_2, and 1370 mbar H_2 over Ni/Cu(100) is shown in Fig. 6. Here, we observe strong changes in the TPD spectra as various amounts of Ni are adsorbed prior to the reaction. At very low coverages. ($\theta_{Ni} = 0.02$ ML) the TPD spectrum is very similar to the spectrum obtained for the clean Cu(100) surface (Fig. 6, bottom curves in both panels). The only qualitative difference we observe is a very small CO-related peak observed at $T = 340$ K. In accordance with the results obtained from the CO/H_2 mixture this is attributed to CO desorption from Ni-related sites. Already at $\theta_{Ni} = 0.10$ ML the TPD spectrum is markedly different. The dominant part of the CO_2-related peak has moved towards lower temperatures and is situated at $T \sim 370$ K. As for the results discussed above, this is attributed to disproportionation of formate bound to one (or more) Ni atoms. Furthermore, the CO-related peak has increased considerably in intensity and shifted towards a higher temperature ($T_{max} = 350$ K). Upon further deposition of Ni we observe a continous increase in the CO-related TPD peak and a shift towards higher temperature, as well as the appearance of an additional TPD feature on

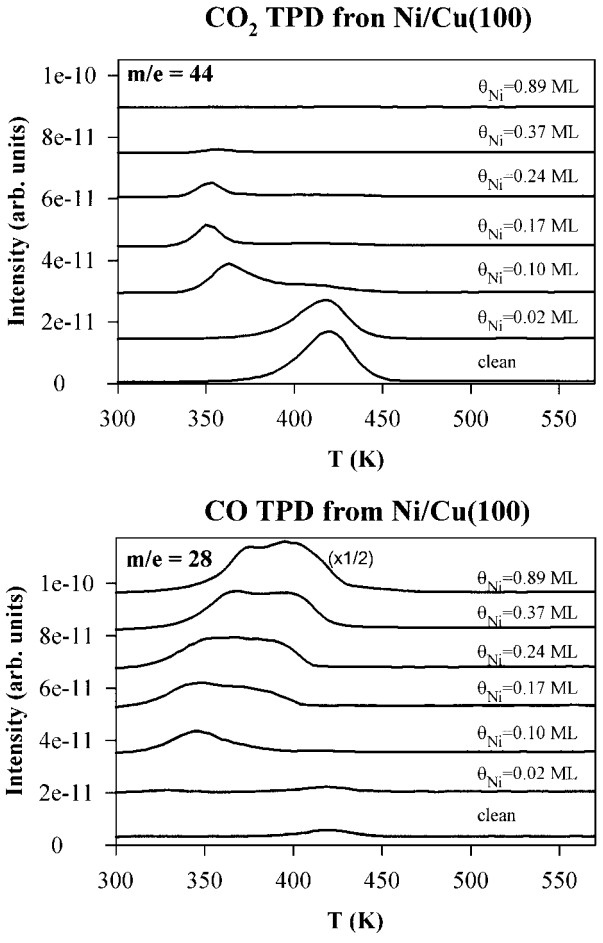

FIG. 6. TPD curves (m/e = 44, upper panel; m/e = 28, lower panel) obtained after reactions involving 100 mbar CO, 30 mbar CO_2, and 1370 mbar H_2 over Ni/Cu(100) at various Ni coverages.

the high-temperature side of the initially observed peak. This feature becomes dominating at higher Ni coverages. This shift towards higher temperatures is also in accordance with what was observed in Ref. (14). Here, it was attributed to an increase in the CO-Ni coordination at increasing Ni coverage.

As mentioned above it was found that even a partial pressure of 0.2 mbar CO in a CO_2/H_2 reaction mixture led to noticeable CO desorption in the postreaction TPD. In order to study this feature in more detail we have obtained a series of TPD spectra after various exposures of CO to a 0.15 ML Ni/Cu(100) surface. Figure 7 (curve a) shows the CO TPD peak obtained after exposing a freshly deposited Ni film to 10 L of CO at RT. The sample was then cooled to RT and reexposed to 10 L of CO. In this case no adsorption of CO takes place (Fig. 7, curve b). This means that no Ni is present at the surface after annealing in UHV to the final temperature of the TPD experiment (which is also the reaction temperature (543 K)). This finding is in accordance with the work of Hernnäs *et al*. (18) who found that extensive migration of Ni into subsurface sites takes place upon annealing at this temperature. If, however, one exposes the post-TPD surface to elevated CO pressures in the HPC for $\Delta t = 15$ min at $T = 320$ K desorption of CO is observed as shown in Figs. 7c–g. It is found that the amount of CO present at the surface depends critically on the partial pressure of CO (Fig. 7, insert). This emphasizes that we are dealing with a gas phase induced surface segregaton of Ni and that it is the CO partial pressure which to a large extent is governing the surface composition of the Ni/Cu(100) system. Already at $P_{CO} = 0.5$ mbar approximately 1/3 of the deposited Ni has been extracted back to the surface. Since the exposure time and temperature (15 min at 320 K) are not far from the situation where the gases are pumped out after a reaction we would expect a similar influence of CO on the postreaction surface concentration of Ni.

Figure 8 shows the $Ni_{2p_{3/2}}$ peak as a function of treatments similar to those of Fig. 7. The lower curve shows the Ni peak just after the Ni deposition at room temperature and a 10-L CO dose. The middle curve displays the same region after a TPD experiment similar to that of Fig. 7, where the crystal was heated to 543 K. The Ni signal was reduced by about 30% by this treatment, implying that the Ni has gone subsurface, in good agreement with the observation that no CO can be adsorbed at room temperature after this experiment. The uppermost curve shows the Ni peak after an exposure to 100 mbar CO for 15 min at 320 K. It is clearly seen that the intensity of the Ni signal is recovered, indicating, as was also illustrated by the TPD curves in Fig. 7,

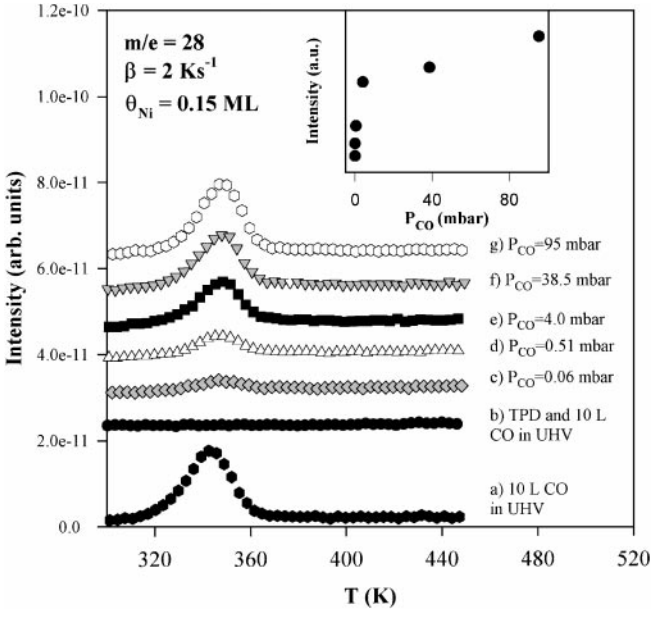

FIG. 7. CO TPD curves (m/e = 28) obtained from 0.15 ML Ni/Cu(100) after (a) a dose of 10 L CO in UHV at RT; (b) a dose of 10 L CO at RT after the first TPD heating to 543 K; and (c)–(f) after dosing at various pressures of CO at $T = 320$ K for $\Delta t = 15$ min (also following a TPD). The insert displays the integrated intensities as funtions of the partial pressure of CO.

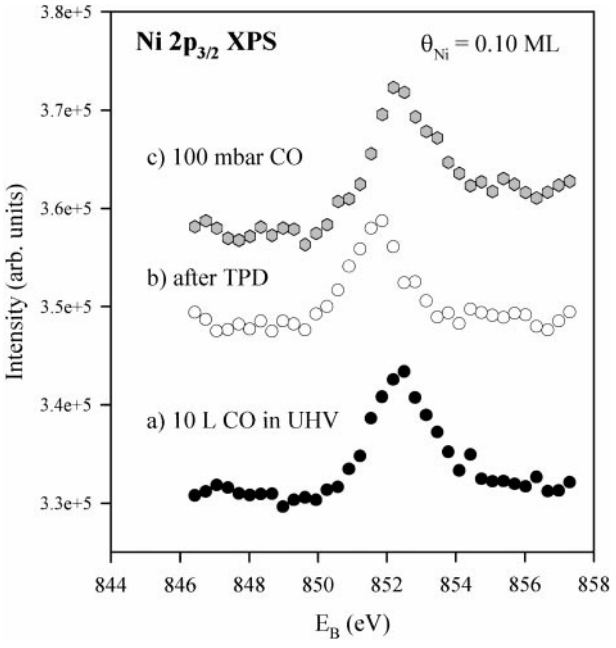

FIG. 8. The $Ni_{2p_{3/2}}$ peak as a function of treatments similar to those of Fig. 7. The lower curve shows the Ni peak just after the Ni-deposition at room temperature and a 10 L CO dose. The middle curve displays the same region after a TPD experiment similar to that of Fig. 7, where the crystal was heated to 543 K. The uppermost curve shows the Ni peak after an exposure to 100 mbar CO for 15 min at 320 K.

that the Ni has been extracted back to the surface. The chemical shift observed due to the CO is in good agreement with the observations by Hernnäs *et al.* (18).

4. DISCUSSION

4.1. Cu(100)

The most central outcome of the present work is the observation that addition of CO to a reaction mixture of CO_2 and H_2 does not lead to a measureable increase in the rate of MeOH formation over Cu(100) (Fig. 1). We do not see any reason why this observation should not hold for clean Cu surfaces in general. As mentioned in the Introduction our finding is nonetheless in opposition to what was observed in Ref. (6), where a small increase in MeOH formation over Cu(110) was observed upon admission of CO to the reaction mixture. This observation was accompanied by a CO-related TPD feature at $T \sim 380$ K, which, according to our results (Fig. 5), is not related to clean Cu. One possibility which would merge the present results with those of Ref. (6) is surface contamination of a species which promotes the MeOH formation (and gives rise to the TPD feature at $T \sim 380$ K). Considering the problems mentioned in the Introduction of Ni contamination that we had to overcome in order to perform the present experiments Ni is indeed a possibility. This suggestion is further supported by the results of Section 3.2 which shows that Ni indeed has a promoting effect on the MeOH synthesis from a mixture of CO, CO_2, and H_2, just as the position of the CO TPD peak introduced by Ni (Figs. 5 and 6) is very similar to what was observed in Ref. (6). By comparison to Fig. 4 the 60% increase in rate upon the addition of CO in Ref. (6) could be attributable to the presence of less than 5% of a ML of Ni impurity in the experiments of Ref. (6). As we show, this could have disappeared into the bulk after postreaction TPD removal of CO, so that it could have been easily unobservable in postreaction XPS if performed after TPD.

Consequently, the present work seems to end the ongoing discussion referred to in the Introduction regarding a possible direct influence of CO on the rate of MeOH formation over Cu-based catalysts. Instead our results indicate that the promoting effect of CO on the rate of MeOH formation observed over real catalysts is more of an indirect nature. The admission of CO has, as we see it, two major consequences, which both relate to the strong change in reduction potential. First, it leads to (reversible) morphology changes as has been demonstrated for Cu/ZnO catalysts by Clausen and co-workers (8). These changes have lately been incorporated in a dynamic microkinetical model by Ovesen *et al.* (9) which led to an improved description of kinetic data of working catalysts. Second, changes in the surface composition of a working catalyst under strongly reducing conditions cannot be ruled out. For instance, it is known that MeOH formation from CO_2 and H_2 over Cu(111) is strongly enhanced upon the deposition of submonolayer quantities of Zn (6). As suggested by Topsøe and Topsøe (19), it can then be speculated that a strongly reducing treatment of a Cu/ZnO catalyst leads to part reduction of ZnO and the subsequent formation of a Zn/Cu surface alloy. According to the authors this would explain the large downward shift in the CO band observed by FTIR for Cu/ZnO catalysts at strongly reducing conditions.

4.2. Ni/Cu(100)

The main observation with respect to methanol formation over Ni/Cu(100) is the establishment of a promotional effect of Ni upon reaction of a mixture containing CO_2, CO, and H_2 (Fig. 4), whereas Ni does not influence the rates obtained from CO/H_2 and CO_2/H_2 mixtures. In order to understand the mechanism behind these observations we turn to the information obtained in Section 3.2, regarding the surface composition of the Ni/Cu(100) system after various treatments.

It should be obvious from the data presented in Section 3.2 that the presence of a partial pressure of CO influences the surface concentration of the Ni/Cu(100) system. This follows both from Fig. 3 and even more clearly from Fig. 7 (insert), which shows that the surface concentration of Ni depends critically on the partial pressure/exposure of CO. According to this no CO can be

adsorbed after an exposure at RT of 10 L ($P_{CO} = 5 * 10^{-8}$ mbar) on a Ni/Cu(100) surface which has been annealed previously at $T = 543$ K in UHV (Fig. 7, curve b). This finding is in agreement with the surface phase diagram of the Ni/Cu system. According to this, Ni and Cu will alloy and Cu will segregate to the surface (20), which will prevent adsorption of CO at RT. It is, however, well established that the chemical potential of the gas phase may alter the surface structure, since strong bonding of adsorbates results in an energy gain of the system (21, 22). For the present system this means that the stronger bonding of CO to Ni, compared to Cu results in the segregation of Ni to the surface.

The strength of the segregational effect obviously depends critically on the CO coverage and thereby on the CO partial pressure, as well as the temperature, just as the kinetics of the diffusion of Ni in Cu should be taken into account for a precise description of the phenomena. The influence of temperature means that the Ni segregation observed at the pump-out temperature (Fig. 7) only reflects the underlying mechanism behind the segregational behavior of Ni in the presence of CO, rather than the actual coverage at the reaction conditions. Owing to the complexity of the system it is difficult to be very specific about the conditions at which the surface segregation occurs. One can estimate the final surface coverage of CO as a function of the CO partial pressure from the sticking coefficient, S_0, and the activation energy, E_a. The resulting coverages obtained for Cu(100) ($E_a = 47$ kJ/mol (23), $S_0 = 0.5$ (24)) and for Ni adsorbed on Cu(100) ($E_a = 96.1$ kJ/mol (obtained from the desorption temperature of CO on Ni/Cu(100)) and, by assumption, $S_0 = 1$) are shown in Fig. 9 for the reaction temperature ($T = 543$ K) and the pump-out temperature ($T = 333$ K). Since Ni is embedded in a Cu matrix and Ni tends to go subsurface if it is not bonding to CO, it is not sufficient only to consider the CO coverage for the Ni/Cu(100) system (Fig. 9, uppermost curves). The CO coverage will also depend on the kinetics, namely the diffusion of Ni and Cu and to what extent there is a chance to meet a CO molecule when the Ni atoms now and then emerge at the surface. The latter will mainly be determined by the CO coverage on the copper. With respect to the reaction conditions the CO coverage on Cu(100) is essentially zero at conditions corresponding to the reaction of CO_2 and H_2 ($P_{CO} \sim 0.2$ mbar). We consider this to be insufficient for the segregational effect to occur at the reaction temperature, although an appreciable Ni coverage could be obtained in the final state according to Fig. 9. In case of a reaction temperature involving 100 mbar CO, we do have a measureable CO coverage on Cu. Since the CO coverage on Ni sites essentially is 1 under these conditions, in the final state this most probably leads to the segregational effect desribed above. It is also understandable that the coverages obtained at the pump-out temperature (333 K) in the case of the reaction of CO_2 and H_2 is noticeable, since already at $P \sim 0.2$ mbar the coverage on Cu(100) is nonzero.

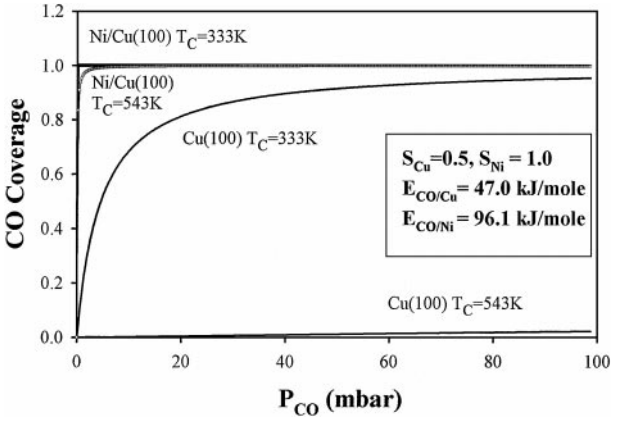

FIG. 9. Calculated curves showing the CO coverage on Cu(100) ($E_a = 47.0$ kJ/mole, $S_0 = 0.5$) and Ni/Cu(100) ($E_a = 96.1$ kJ/mole, $S_0 = 1$) as functions of the partial pressure of CO at $T = 333$ K (pump-out temperature) and $T = 543$ K (reaction temperature).

From the above discussion it follows that the admission of CO to the synthesis gas most probably results in the maintenance of Ni at the surface in the Ni/Cu(100) system, whereas this is not facilitated when CO is not admitted to the surface. Thus, we can understand the promotional effect of Ni in case of a $CO/CO_2/H_2$ mixture, as well as the unpromotional effect in the case of the CO_2/H_2 mixture, as a result of CO-induced surface segregation of Ni in the first case while this is not obtained in the second case.

Having established the nature of the promotional effect we should finally address the underlying reaction mechanism. In principle, two possibilities exist. Either MeOH is formed exclusively from CO_2 and H_2 also over Ni/Cu(100) or an additional pathway, the direct hydrogenation of CO, is opened by the presence of Ni at the surface. We have addressed this issue in more detail in another report (25). Some indications can, however, be obtained from the present work. For instance, the possibility of direct hydrogenation of CO appears not to be very likely in case of the Ni/Cu(100) system, owing to the fact that MeOH cannot be formed from CO and H_2 alone in this system (Section 4.2.). One can, of course, not exclude a priori that CO_2 can act as a promotor in this system, but it is not at all clear what the role of CO_2 could possibly be in this case. On the other hand, it is much more reasonable to consider a strictly promoting role of CO, when one considers the segregational behavior of Ni in the presence of a partial pressure of CO. It is obvious from the difference in the formate TPD spectra of Fig. 6 (upper panel) that the surface is becoming much more reactive when depositing Ni, leading to a lower decomposition temperature of the formate. It is, therefore, also to be expected that the Ni will have some strong influence on the rate-limiting step for the synthesis of methanol from CO_2 and H_2 (5, 25). One way of getting definite proof

of this would be by returning to a QMS-based analysis of the reaction mixture and by conducting experiments involving isotopic labelled C^{13}.

5. CONCLUSION

It is found that CO does not influence the rate of MeOH formation from CO_2 and H_2 over clean Cu(100). Apparently, this finding excludes that direct hydrogenation of CO plays a role in MeOH formation over Cu-based catalysts. Instead, the promoting role of CO in these catalysts most probably relates to the change in reduction potential of the synthesis gas introduced by the presence of CO. This change can lead to both morphology changes, as well as changes in the surface composition.

In case of the Ni/Cu(100) system it is found that the deposition of submonolayer quantities of Ni does not lead to changes in the rate of MeOH formation from mixtures containing CO_2 and H_2, just as MeOH cannot be formed in measureable amounts from CO/H_2 admixtures over Ni/Cu(100). In the first case Ni will simply not be present on the surface and in the latter case it is not capable of hydrogenating CO. On the other hand, deposition of Ni leads to a dramatic increase in the rate of MeOH formation from mixtures containing all three components, CO, CO_2, and H_2, with the initial TOF/Ni site $\sim 60 \times$ TOF/Cu site. It is found that the admission of CO to the synthesis gas is necessary in order to maintain Ni at the surface. It is suggested that CO acts purely as a promotor in the system and, consequently, we ascribe the increase in activity to a promotion through gas phase induced surface segregation of Ni.

ACKNOWLEDGMENTS

This work was founded by the Center for Atomic-scale Materials Physics (CAMP), financed by the Danish National Research Foundation and the Center for Surface Reactivity, financed by the Danish Research Councils.

REFERENCES

1. Kagan, Y. B., Liberov, L. G., Slivinski, E. V., Moloktev, S., Lin, G. I., Rozovski, A. Y., and Bashkirov, A. N., *Dokl. Akad. Nauk. SSR* **221**, 1093 (1975).
2. Bowker, M., Houghton, H., and Waugh, K. C., *J. Chem. Soc. Faraday Trans. I* **77**, 3023 (1981).
3. Chinchen, G. C., Denny, P. J., Parker, D. G., Spencer, M. S., Waugh, K. C., and Whan, D. A., *Appl. Catal.* **30**, 333 (1987).
4. Rasmussen, P. B., Kazuta, M., and Chorkendorff, I., *Surf. Sci.* **318**, 267 (1994).
5. Rasmussen, P. B., Holmblad, P. M., Askgaard, T., Ovesen, C. V., Stoltze, P., Nørskov, J. K., and Chorkendorff, I., *Catal. Lett.* **26**, 373 (1994).
6. Yoshihara, J., and Campbell, C. T., *J. Catal.* **161**, 776 (1996).
7. Nakamura, J., Nakamura, I., Uchijima, T., Watanabe, T., and Fujitani, T., *Stud. Surf. Sci. Catal.* **101**, 1389 (1996).
8. Clausen, B. S., Schiøtz, J., Gråbæk, L., Ovesen, C. V., Jakobsen, K. W., Nørskov, J. K., and Topsøe, H., *Topics in Catal.* **1**, 367 (1994).
9. Ovesen, C. V., Clausen, B. S., Schiøtz, J., Stoltze, P., Topsøe, H., and Nørskov, J. K., *J. Catal.* **168**, 133 (1997).
10. Chorkendorff, I., and Rasmussen, P. B., *Surf. Sci.* **248**, 35 (1991).
11. Chorkendorff, I., Wambach, J., and Nerlov, J., *J. Appl. Catal. A*, to appear.
12. Askgaard, T., Nørskov, J. K., Ovesen, C. V., and Stoltze, P., *J. Catal.* **156**, 229 (1995).
13. Taylor, P. A., Rasmussen, P. B., Ovesen, C. V., Stoltze, P., and Chorkendorff, I., *Surf. Sci.* **261**, 191 (1992).
14. Yu, K. Y., Ling, D. T., and Spicer, W. E., *J. Catal.* **44**, 373 (1976).
15. Wambach, J., Illing, G., and Freund, H.-J., *Chem. Phys. Lett.* **184**, 239 (1991).
16. Nakamura, J., Rodriquez, J. A., and Campbell, C. T., *J. Phys.* **149**, 1 (1989).
17. Rasmussen, P. B., Taylor, P. A., and Chorkendorff, I., *Surf. Sci.* **269/270**, 352 (1992).
18. Herrnäs, B., Karolewski, M., Tillborg, H., Nilsson, A., and Mårtensson, N., *Surf. Sci.* **302**, 64 (1994).
19. Topsøe, N.-Y., and Topsøe, H., *J. Mol. Catal.*, in press.
20. Christensen, A., Ruban, A. V., Stoltze, P., Jacobsen, K. W., Skriver, H. L., Nørskov, J. K., and Besenbacher, F., *Phys. Rev. B* **56**, 5822 (1997).
21. Ponec, V., *Surf. Sci.* **80**, 352 (1979).
22. Tomànek, D., Mukherjee, S., Kumar, V., and Bennemann, K. H., *Surf. Sci.* **114**, 11 (1982).
23. Pope, T. D., Griffiths, K., and Norton, P. R., *Surf. Sci.* **306**, 294 (1994).
24. Harendt, C., Goschnick, J., and Hirshwald, W., *Surf. Sci.* **152/153**, 453 (1985).
25. Nerlov, J., and Chorkendorff, I., *Catal. Lett.* **54**, 171 (1998).